Available online at www.sciencedirect.com
ScienceDirect
Journal of Luminescence 128 (2008) 1431–1441
JOURNAL OF LUMINESCENCE
www.elsevier.com/locate/jlumin

Effect of metal salts in the optical properties of polydiacetylenes

J.A. Díaz-Ponce[a], O.G. Morales-Saavedra[b,*], M.F. Beristaín-Manterola[a], J.M. Hernández-Alcántara[c], T. Ogawa[a]

[a]*Instituto de Investigaciones en Materiales, IIM-UNAM, Universidad Nacional Autónoma de México, P.O. Box 70-360, 04510 México D.F., México*
[b]*Centro de Ciencias Aplicadas y Desarrollo Tecnológico, CCADET-UNAM, Universidad Nacional Autónoma de México, P.O. Box 70-186, 04511 México D.F., México*
[c]*Instituto de Física, IF-UNAM, Universidad Nacional Autónoma de México, P.O. Box 20-364, 01000 México D.F., México*

Received 15 October 2007; received in revised form 21 January 2008; accepted 24 January 2008
Available online 5 February 2008

Abstract

Films of polydiacetylene (PDA)-containing polyesters with metal salts of Zn, Eu and Gd were prepared. Ultraviolet–visible (UV–VIS) absorption and photoluminescent (PL) spectra indicated that the presence of the metal salts induced a small shift of their maxima to higher and lower energies, respectively. PDAs films with an ester group in allylic position to the conjugated system presented two emission bands. The higher energy emission band was assigned to carbonyl emission and the lower energy emission band to self-trapped excitons (STE). Indeed, the inclusion of metal salts incremented the intensity relation between the higher and lower emission energy bands. On the other hand, Raman spectroscopy measurements performed in PDAs films derived of pentyn-1-ol indicated that the metal salts induced a slight statistical shift in the triple and double bond signals to higher energies. In this way, the intensity variations and band shifts detected by Raman, UV–VIS and PL spectroscopies showed that the presence of metal salts could have a remarkable influence on the energy levels of these PDAs. Nonlinear optical (NLO) third harmonic generation (THG) measurements were performed in order to verify this affirmation as well as the cubic NLO performance of these materials.

PACS: 78.55.Qr; 81.05.Ni; 82.35.Ej: 85.40.Xx

Keywords: Polydiacetylene; Metal salt; Films; Optical properties; NLO; THG

1. Introduction

Polydiacetylenes (PDAs) are conjugated polymers with one-dimensional electronic properties. The conjugation length of PDAs causes the presence of absorption bands in the visible spectra, but luminescence is generally not found in PDAs, because the lowest excited energy level is 2Ag, which has a non-radiative transition to the ground level 1Ag. However, some PDAs have shown luminescence [1–5], in this case the lowest excited level is 1Bu, which has a radiative channel to the ground level 1Ag. Quantum yields as high as 10^{-2} have been reported [6]. This change in energy levels is associated with disorder in PDAs [1,2]. On the other hand, metal salts such as TiO_2, Al_2O_3, ZnO, CdS and CdSe have been added to conjugated polymers such as PPV, MEH–PPV and CN–PPP and their effect on the luminescence of these conjugated polymers has been studied [7–9].

The great delocalization of the π-conjugated electrons in PDAs produces large values of the cubic nonlinear optical (NLO) susceptibility $\chi^{(3)}$. Potential technological applications of PDAs, such as optical switching and waveguiding devices, require appropriate transparency in the visible region of these materials and processability to be adapted in integrated optical devices, where a fast optical response (sub-picoseconds) is usually required [10–12]. On the other hand, organometallic compounds are commonly implemented to increase the hyperpolarization of organic conjugated materials through the electronic density

*Corresponding author. Tel.: +52 55 56 22 86 02x1124; fax: +52 55 56 22 86 37.
E-mail addresses: omar.morales@ccadet.unam.mx, omardel@gmail.com (O.G. Morales-Saavedra).

0022-2313/$ - see front matter © 2008 Elsevier B.V. All rights reserved.
doi:10.1016/j.jlumin.2008.01.013

transfer between the metal atom and the organic conjugated system [13]. In this way, PDAs have been coordinated to Co, Mo and W [14], Ag [15] and Au [16]. In some cases, the values of the NLO $\chi^{(3)}$-coefficients are successfully perturbed [14]. In addition, Ogawa et al. [17] have added metal salts of Gd and Eu to PDA-containing aromatic polyamides and the NLO properties were increased. This coordination is not limited to the conjugated system; the metal compounds may interact with the side groups of these polymers and produce a homogeneous distribution of these compounds. Ionic groups such as carboxylates are commonly implemented in these polymers [15,16,18–20]. Neutral groups like amines [21–25] and amides [26] are also utilized. For these reasons, films of aliphatic PDA-containing polyesters with metal salts of Zn, Eu and Gd were prepared, and the influence of these metal salts in the optical properties of the developed PDA films is extensively discussed within this work. The polyester films were selected due to their adequate transparency and high NLO values [27]. Measurable band shifts from the Ultraviolet–visible (UV–VIS) absorption, photoluminescent (PL)- and Raman-spectra were detected by the interaction with the metal salts. These facts, associated with the localization of the electronic charge, were related to a decrement of the cubic NLO properties of the studied samples. It was also found that if the metal salt increases the conjugation of PDAs through its interaction with their side group, the cubic NLO properties are also incremented.

2. Experimental

2.1. Diacetylene synthesis and characterization

Dichloromethane, dimethylformamide (DMF), propargyl alcohol, 4-pentyn-1-ol and triethylamine were dried and distilled. *o*-Dichlorobenzene and N,N,N′,N′ tetramethylethylendiamine (TMEDA) were distilled. Cuprous chloride CuCl (+98%) was purified by dissolution in concentrated HCl, followed by precipitation with water, filtration, washing with ethanol and acetone and drying under vacuum at 100 °C. Methanol and thionyl chloride (Fluka) were used as received; the remainder of the previous substances was supplied by Aldrich (reactive grade). Metal salts of $ZnCl_2$, $EuCl_3\ xH_2O$ and $GdCl_3\ 6H_2O$ (GSF-Chemicals) were used as starting materials in order to form the composites. Wide angle X-ray scattering (WAXS) measurements were performed by means of a Brucker-axs D8-Advance system, with radiation of Cu K_α at 1.540 Å. Percentage of crystalline area was considered as the percentage of crystallinity. The weight-average molecular weight (Mw) and the polydispersity index (PI) were determined by gel permeation chromatography (GPC, using tetrahydrofuran: THF, Baker, HPLC grade) as eluent. The synthesis of the diacetylene-containing polyesters poly(2,4 hexadyin-1,6-ylene azelate) PHDAz and poly(4,6 decadyin-1,10-ylene azelate) PCDAz was performed according to the following procedure [28,29]: azelaoyl chloride was obtained from the reaction of 50.0 g (265.6 mmol) of azelaic acid and 94.8 g (796.9 mmol) of thionyl chloride with DMF (traces) as catalyst and 200 mL of dichloromethane as solvent at room temperature for 48 h. The reaction mixture was then distilled at reduced pressure to obtain pure azelaoyl chloride. The 10.0 g (44.4 mmol) of this product was reacted with 97.7 mmol of the acetylenic alcohol (propargyl alcohol to obtain PHDAz or 4-pentyn-1-ol to obtain PCDAz) in 150 mL of dichloromethane as solvent at room temperature in order to obtain the respective bisacetylenic monomer. Triethylamine (9.4 g, 92.4 mmol) was used as catalyst and proton acceptor. After 24 h, the reaction mixture was rotoevaporated and left at high vacuum. Then 50 mL of acetone was added and the mixture was filtered and distilled at reduced pressure to obtain the pure bisacetylenic monomer. The diacetylene-containing polyesters (PHDAz or PCDAz) were obtained by Glaser oxidative coupling modified by Hay [30]: 2 g of these bisacetylenic monomers were added to 6 mL of *o*-dichlorobenzene, afterwards 0.17 g (1.7 mmol) of the CuCl catalyst and 0.3 mL (2.0 mmol) of the co-catalyst TMEDA were also added to the solution. The polymer was precipitated from the reaction mixture by addition of acidified methanol with concentrated HCl 3% (v/v). Afterwards, the polymer was vacuum dried at room temperature. PHDAz and PCDAz crystallinities were 28.4% and 26.2%, respectively. It is considered that the conversion to the corresponding PDAs depends on this percentage [31]. The diacetylene-containing polyesters were soluble in dichloromethane, THF and DMF. PHDAz had an Mw of 16,100 g/mol with a PI of 3.4. PCDAz had an Mw of 55,952 with a PI of 4.9.

2.2. PDA film preparation and characterization methodology

Films were prepared by solution casting and spin coating with DMF as solvent and deposited on fused silica glass substrates. For Raman, WAXS and IR measurements, the films were deposited on Teflon and then detached. The concentration of the diacetylene solution was 17 g/L in solution casting and up to 166 g/L in spin coating. Solution casting conditions were 50 °C, 23 in. Hg of vacuum pressure and 3 h of film evaporation–annealing time. Spin coating conditions were varied from 30 to 50 °C and from 1000 to 1700 rpm. These films were UV-irradiated by means of a 400 W mercury lamp for 15 min in order to achieve the respective PDAs by topochemical polymerization. Fig. 1 shows the structure of the PDAs, where the triple bond is conjugated with the double bond (enyne structure). When $n = 1$, we have the structure of PDA–PHDAz, in which the ester group is in allylic position to the conjugated system. This had consequences in the optical properties of this PDA, as is analyzed later in this work.

Film thickness was measured by a profilometer (Sloan Dektak IIA, 50 Å resolution). Determination of the metal percentage within the films was performed by X-ray

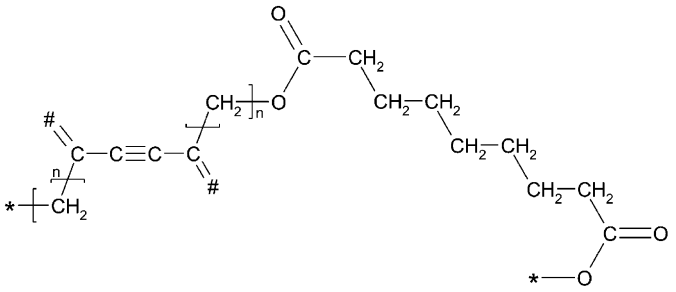

Fig. 1. Structure of PDA-containing polyesters: PDA–PHDAz ($n = 1$) and PDA–PCDAz ($n = 3$). The hash signs indicate a repetition of the structure in the double and triple bonds. The asterisk signs in methylene and oxygen indicate a repetition of the structure with the joining of the methylene to another oxygen of an ester group and vice versa.

photoelectron spectroscopy (XPS). XPS-measurements were carried out on selected samples in a high vacuum system (UHV; VG-Scientific Michrotech ESCA-2000) with an X-ray source of Al K_α ($h\nu = 1453.6$ eV). Energy position was calibrated with the photopeak of Ag $3d^{5/2}$ in the position of 367 eV, with a resolution of full-width at half-maximum (FWHM) of 1.0 eV. The absorption spectra of the samples were obtained from a Milton Roy S spectrophotometer (Spectronic 3000, 1 nm resolution), using a fused silica glass substrate as the reference. The PL spectra of the samples were recorded on a Perkin Elmer fluorimeter (650–10S, 2 nm resolution); samples were placed in a parallel geometry to the incident beam. The vitreous transition temperature (Tg) was determined by differential scanning calorimetry (DSC) experiments, performed in a Dupont Instrument 2910 under N_2-atmosphere with a heating rate of 10 °C/min. Raman measurements were obtained with the Almega XR dispersive Raman system, equipped with an Nd:YVO_4 laser system frequency doubled to $\lambda = 532$ nm (2.33 eV). Samples were excited with ~2.0 mW. This system has an integrated Olympus BX51 microscope where 10× and 50× objectives were used to focus the laser beam on the sample. The same objectives were implemented to collect the back-scattered light. The detector system consisted of a CCD camera thermoelectrically cooled to −50 °C and a monochromator device with 675 and 2400 line/mm gratings, which provided a resolution of ~4 and ~1 cm^{-1}, respectively. Finally, selected samples were also studied as active media for NLO-effects such as third harmonic generation (THG); for this propose, a commercial Q-switched Nd:YAG laser system, operating at $\lambda_\omega = 1064$ nm with a repetition rate of 10 Hz and a pulse width of $\tau = 12$ ns (Continuum-Surelite II) was implemented to provide the fundamental wave. Typical pulse powers of 200 μJ were implemented in order to irradiate the film samples, with a variable intensity on the sample that ranged from 30 to 50 MW/cm^2 and controlled by neutral density filters in order to avoid laser induced damage caused by high intensities of strong focused beams. It was possible to select the desired polarization of the fundamental beam by means of an IR-coated Glan-Taylor polarizer and a quartz-retarder ($\lambda/2$-plate, zero-order). A second polarizer was used as an analyzer, allowing the characterization of the THG light. The third harmonic wave ($\lambda_{3\omega} = 355$ nm) was detected by a sensitive photomultiplier tube (PMT-Hamamatsu, R-928) behind optical interference filters centered at 355 ± 5 nm. The THG device was calibrated by means of a fused silica plate ($\chi^{(3)} = 3.11 \times 10^{-14}$ esu, at $\lambda_\omega = 1064$ nm), which is frequently used as standard NLO reference via the Maker-Fringes method for THG experiments.

3. Results and discussion

3.1. Optical properties of PDA films

Films of PDA–PHDAz prepared by solution casting were orange colored, whereas films of PDA–PCDAz prepared by spin coating were blue colored. All the film samples were homogeneous and adequately transparent in the visible spectral region. Transparency of these films with metal salts was obtained at 5% w/w with respect to the diacetylene. Solutions at 10% w/w gave films with a white halo; these concentrations were ideal because a portion of the metal salts precipitated when the solutions were prepared. The orange PDA–PHDAz film thickness varied from 2.0 to 4.9 μm and the blue PDA–PCDAz film thickness varied from 3.2 to 3.7 μm. The XPS-measured metal ion concentration was up to 4 times larger than that of the original metal concentration in the solution. Therefore, it is considered that there was a migration of the metal salt to the surface of the film [32]. A percentage of nitrogen was also found on the surface of the films, probably due to the displacement of water molecules placed on the metal coordination sphere caused by the interaction of DMF molecules [33,34].

3.2. UV–VIS absorption spectra

Fig. 2 shows the absorption spectra of the orange PDA–PHDAz films with maxima at 465 and 500 nm. The absorption maximum at 500 nm (2.48 eV) corresponds to the free excitonic transition 1^1Bu and the maximum at

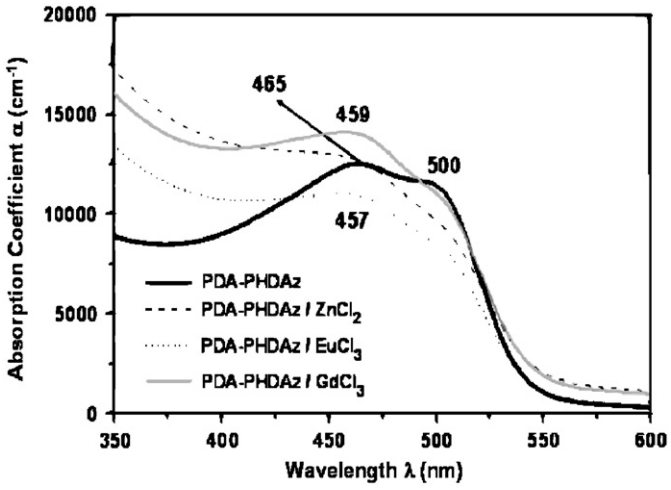

Fig. 2. UV–VIS absorption spectra of orange PDA–PHDAz films with different metal salts.

465 nm (2.67 eV) to the vibronic transition due to the coupling of the excitonic transition with the strengthening of the double bond. This produces a difference in the wavelength of ~35 nm (0.187 eV; 1505 cm^{-1}).

The absorption maximum at 465 nm of orange PDA–PHDAz films containing metal salts shows a small measurable shift to higher energies (~6 nm). This indicates less electron delocalization of the conjugated PDAs produced by the interaction with the metal salt, which could affect the polarizability of the π-conjugated system of PDAs and then the NLO properties. This blue shift was observed in PDAs coordinated with $Co_2(CO)_6$ [14] and also in nanocomposites of PDAs with carboxylate anions coordinated in their side groups with Ag^{1+} cations [15]. The difference in the absorption coefficients (α) in these films is associated with a different conversion from diacetylenes DAs to PDAs. Moreover, Fig. 2 also shows that the absorption maximum at 500 nm of the orange PDA–PHDAz reference films does not have an appreciable shift due to the interaction with the metal salts.

Fig. 3 shows the absorption spectra of blue PDA–PCDAz films with maxima at 580 nm (2.14 eV) and 627 nm (1.98 eV). The absorption band at 627 nm corresponds to the excitonic transition, whereas the band at 580 nm to the vibronic transition. The difference in the wavelengths of 47 nm (0.16 eV; 1292 cm^{-1}) is not assigned to the vibration of the double bond. On the other hand, the interaction with the metal salts produced a small shift of the maxima at 580 and 627 nm to higher energies (~4 nm), less pronounced than that for the orange PDA–PHDAz samples. It is then suggested that a larger blue shift is produced by the metal salt interaction if the energy of the absorption maxima is higher.

3.3. PL spectra

Fig. 4 shows the emission spectra of orange PDA–PHDAz films with $\lambda_{ex} = 250$ nm. These spectra exhibit two emission bands, because the reference sample maxima are located at 394 nm (3.15 eV) and at 565 nm (2.19 eV). These bands in PDAs have been associated with the presence of two population chains [3] with different conjugation length. In this way, the higher energy band at 394 nm could correspond to the emission of short conjugated chains [35] or, as we corroborate later, to the emission of the carbonyl group [36], whereas the lower energy band at 565 nm corresponds to the emission of long conjugated chains. PDAs luminescence bands at lower energies than the exciton have been associated with self-trapped excitons (STE), which are due to the distortion of the polymer induced by the exciton transition [1,37].

Indeed, for films containing metal salts, we observe a change in the relative intensity of the bands at 565 and 394 nm. The band intensity at 565 nm is diminished in relation to the band intensity at 394 nm. In the hypothesis of short conjugated chains, this implies that the metal salts did not allow the STE formation or did not allow the formation of long conjugated chains, or both conditions simultaneously, and then the proportion of shorter conjugated chains emitting at 394 nm was increased. In the hypothesis of the emission of the carbonyl group, this implies that the metal salt did not allow the STE formation and then the intensity of the lower energy emission band is diminished. It is also possible that a strong energy transfer took place from the STE to the metal salt, and from it to other molecules with a subsequent non-radiative relaxation [38]. On the other hand, the emission band at 394 nm shows a shift of up to 10 nm to lower energies due to the interaction with the metal compound; in this case, the Eu salt caused the largest shift. In the hypothesis of carbonyl emission, this implies an interaction between the metal salt and the carbonyl group. For the emission band at 565 nm, the largest shift to lower energy was produced by the Gd metal salt. It is considered that the metal salts affect the

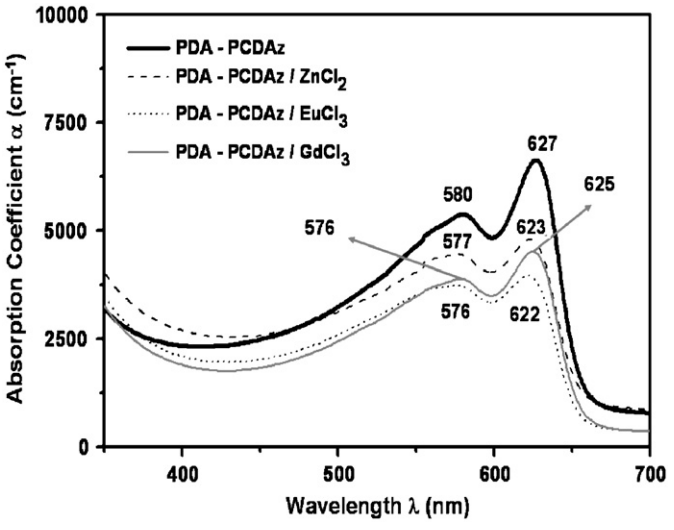

Fig. 3. UV–VIS absorption spectra of blue PDA–PCDAz films with different metal salts.

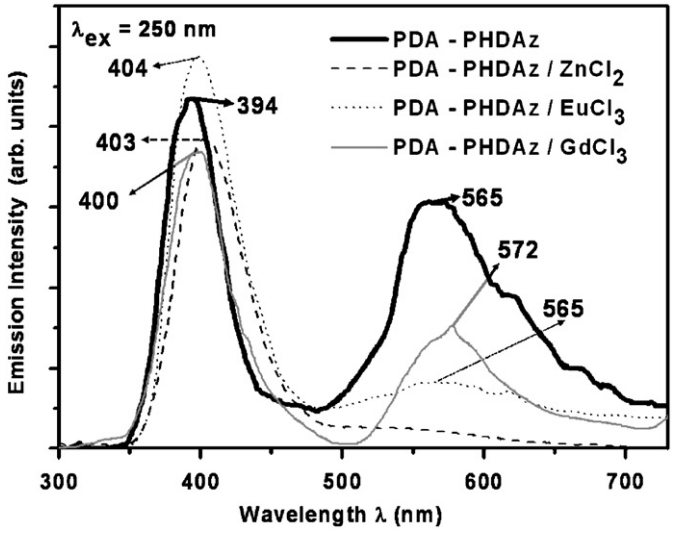

Fig. 4. Emission spectrum at room temperature ($\lambda_{ex} = 250$ nm) for the orange PDA–PHDAz reference and metal salt prepared films.

energy levels of the polymer and, in the emission case, the difference of energy between the excited and the ground level is diminished. Excitation spectra at $\lambda_{em} = 390$ nm (3.18 eV) and $\lambda_{em} = 400$ nm (3.10 eV) of orange PDA–PHDAz films were also obtained (not shown here). The spectra of the orange PDA–PHDAz reference sample and the PDA–PHDAz + metal salts based film composites, presented the same excitation maximum at 250 nm (4.96 eV). This indicates that the emission maximum, but not the excitation maxima, was changed by the presence of metal. In order to clarify if the emission band at 394 nm was produced by the short conjugated chains or by the carbonyl group, we recorded the emission and excitation spectra of the non-UV-irradiated (without color) PHDAz reference film at $\lambda_{ex} = 250$ nm and $\lambda_{em} = 394$ nm, respectively. We observed the characteristic emission and excitation band maxima at 395 and 250 nm of the UV-irradiated orange PDA–PHDAz reference films. We assume then that the carbonyl group, which does not change by the irradiation, produced the luminescence. If the short conjugated chains produced the emission, we should observe a shift of the 250 nm excitation maximum to lower energy with the UV-irradiation (due to the increment of the chain length conjugation of the PDA).

Fig. 5 shows the excitation spectra at $\lambda_{em} = 565$ nm of the orange PDA–PHDAz reference film and films containing metal salts. These excitation spectra show a maximum at 467 nm (2.66 eV), which corresponds to the vibronic excited state, demonstrating that the conformation of this excited state had an influence on the conformation of the formed STE and then over its luminescence as was pointed out by Yoshizawa [1]. The presence of different metal salts did not shift this maximum. This fact implies that the excitation state, precursor of the STE, was not affected, but the conformation of the STE was strongly affected.

Fig. 5 also shows the overlap of the emission band at 394 nm ($\lambda_{ex} = 250$ nm) and the excitation band at 467 nm ($\lambda_{em} = 565$ nm). This indicates an energy transfer between the carbonyl group and the long conjugated chains. For this reason, the excitation spectra at $\lambda_{em} = 565$ nm does not show a maximum at 250 nm, although the emission spectrum at $\lambda_{ex} = 250$ nm shows a maximum at 565 nm (see Fig. 4). Emission spectra with λ_{exc} at the maxima of the UV-absorption spectra were also carried out. Accordingly, Fig. 6 shows the emission spectra at $\lambda_{ex} = 466$ nm of orange PDA–PHDAz films with metal salts, which do not have an appreciable change in the emission band intensity at 565 nm in comparison to that of the reference film. It is considered that when these films were excited at 466 nm, the perturbation of the metal salt was minimized. Indeed, it is observed that the emission maxima are slightly shifted to lower energies in relation to the PL-emission at $\lambda_{ex} = 250$ nm as is shown in Fig. 4.

Fig. 7 shows the emission spectra at $\lambda_{ex} = 500$ nm of orange PDA–PHDAz films, here the interaction with the metal salts provoked an intensity decrement of the emission band at 565 nm. This indicates that the formation of the STE was more affected when the excitation light energy was different to that of $\lambda_{ex} = 467$ nm. This decrement is larger at $\lambda_{ex} = 500$ nm. We consider that at this wavelength, the energy was not enough to break the perturbation caused by the metal salt.

Fig. 8 shows the emission spectra of blue PDA–PCDAz films with $\lambda_{ex} = 240$ nm. An emission band of PDA–PCDAz with a maximum at 395 nm (3.14 eV) is observed. We consider that this band is related to that at 394 nm of the orange PDA–PHDAz films. Indeed, Fig. 8 also shows the excitation spectra with $\lambda_{em} = 400$ nm of blue PDA–PCDAz films (excitation spectra with $\lambda_{em} = 390$ nm were also performed, not shown here), both measurements exhibit

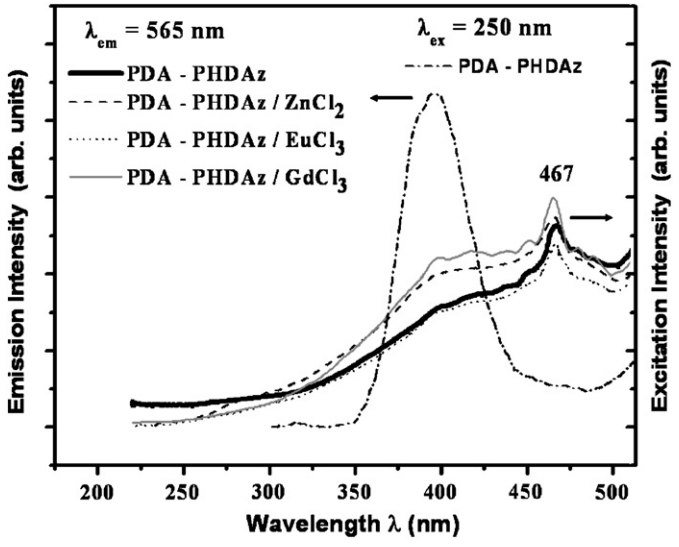

Fig. 5. Emission spectrum at room temperature ($\lambda_{ex} = 250$ nm) for the PDA–PHDAz reference film without the metal salt, which shows the band at 394 nm; and excitation spectra at room temperature ($\lambda_{em} = 565$ nm) for films of the same polymer with different metal salts.

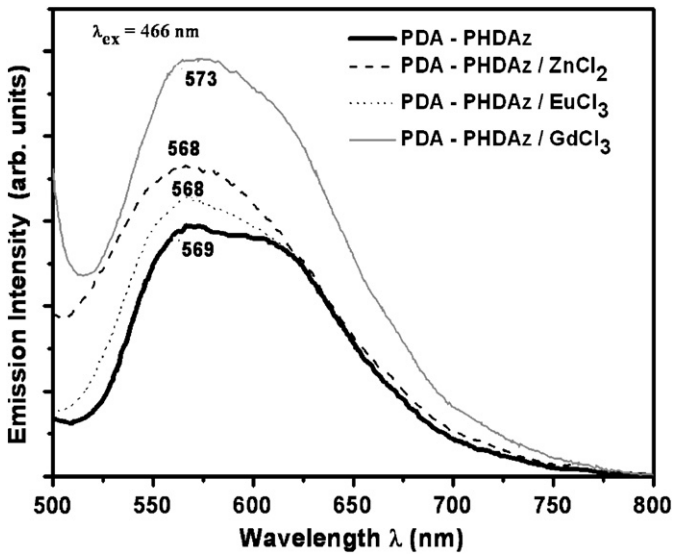

Fig. 6. Emission spectra at room temperature ($\lambda_{ex} = 466$ nm) of orange PDA–PHDAz films with different metal salts.

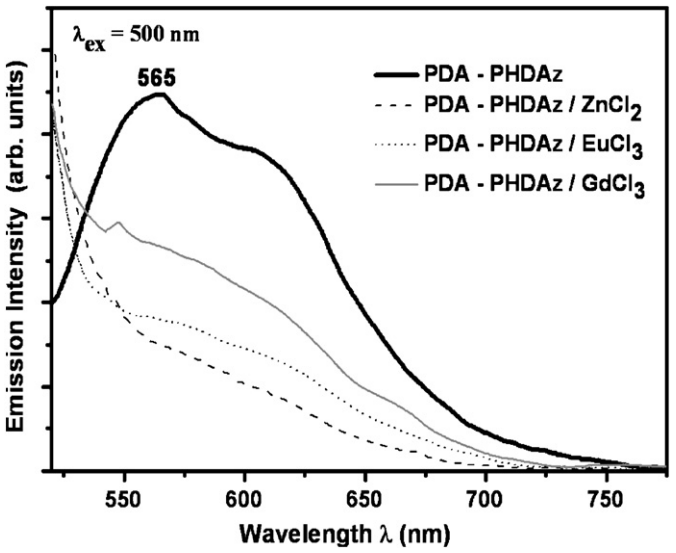

Fig. 7. Emission spectra at room temperature ($\lambda_{ex} = 500$ nm) of orange PDA–PHDAz films with different metal salts.

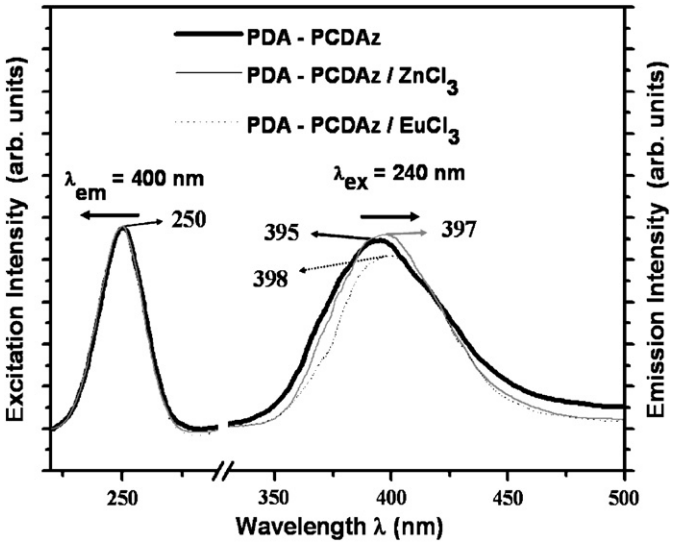

Fig. 8. Excitation spectra at room temperature ($\lambda_{em} = 400$ nm) for PDA–PCDAz films with different metal salts and emission spectra at room temperature ($\lambda_{ex} = 240$ nm) of the same films.

an excitation maximum at 250 nm, which was also present for the orange PDA–PHDAz films. Thus, the emission band at 395 nm is due to the carbonyl group. This band was not appreciably shifted by the interaction with the metal salt in opposition to the orange PDA–PHDAz films. This fact is probably due to the presence of the ester-group in the allylic position for the orange samples. On other hand, the excitation maxima observed at 250 nm for both orange and blue PDAs corresponding to the higher emission bands, were not shifted by the interaction with the metal salts. The same phenomenon also occurred with the excitation maximum observed at 466 nm corresponding to the lower emission band of the orange films.

3.4. Raman spectra

Raman spectroscopy measurements were performed at low and at high resolution (~4 and ~1 cm^{-1}, respectively) in order to analyze if the metal salts had an effect on the double and triple bonds of these PDAs. The best determination of the peak assigned to the triple bond in orange PDA–PHDAz films was obtained at low resolution. On the other hand, the best Raman peak separation in the blue PDA–PCDAz films was obtained at high resolution. For this reason, the Raman spectra of the orange and blue films are reported at the previous best experimental conditions. In this way, Fig. 9a shows the Raman spectrum of the orange PDA–PHDAz reference sample, which exhibits the double bond vibration at 1524 cm^{-1} (0.189 eV), differing from the double bond vibration determined in the absorption spectrum of this film (35 nm; 1505 cm^{-1} in Fig. 2). This is explained because the double bond vibration observed in the Raman spectra belongs to the ground electronic level, whereas the double bond vibration determined in the absorption spectra belongs the excited electronic state. Fig. 9b shows that the interaction of these orange PDA–PHDAz films with the metal salt of Zn did not produce an appreciable shift of the double and triple bond Raman signals. The same behavior occurred with the other metal salts (not shown here for simplicity). Fig. 9c shows the two adjoined resolved bands associated with the double bond vibration of the blue PDA–PCDAz reference sample. One of the bands shows a maximum at 1447 cm^{-1} and the other at 1515 cm^{-1}. The band at 1447 cm^{-1} was produced by the coupling of the double bond vibration with the scissor vibration mode of the enyne adjacent CH_2 group. The band at 1515 cm^{-1} corresponds to the double bond vibration without that coupling [39]. Raman experiments, performed at 28 randomly selected spots of the blue PDA–PCDAz films, showed a broad dispersion of the frequency maxima of these bands, where the first band presented dispersion from 1446 to 1449 cm^{-1} and the second band presented dispersion from 1480 to 1515 cm^{-1}. Moreover, the band maxima associated with the triple bond varied from 2082 to 2107 cm^{-1}. It is affirmed that this variation is produced by the internal strain between the monomer and polymer phases in PDAs. The strain is stronger at low conversions. The strain contributes with additional energy to the vibration, and the Raman signal frequency is reduced [39]. The non- and moderate-UV-irradiated blue PDA–PCDAz films (considered as films at low and high conversion, respectively) showed a similar range of maximum dispersion. This indicates that the range of strain distribution was similar at those conversions in these PDA-containing polyesters, which were different to the PDAs analyzed by Batchelder [39]. On the other hand, the 28 random experimental spots of blue PDA–PCDAz films with metal salt of Zn showed that the presence of the metal salt produced a reorganization of the double and triple Raman maxima distribution, shifting the mean value

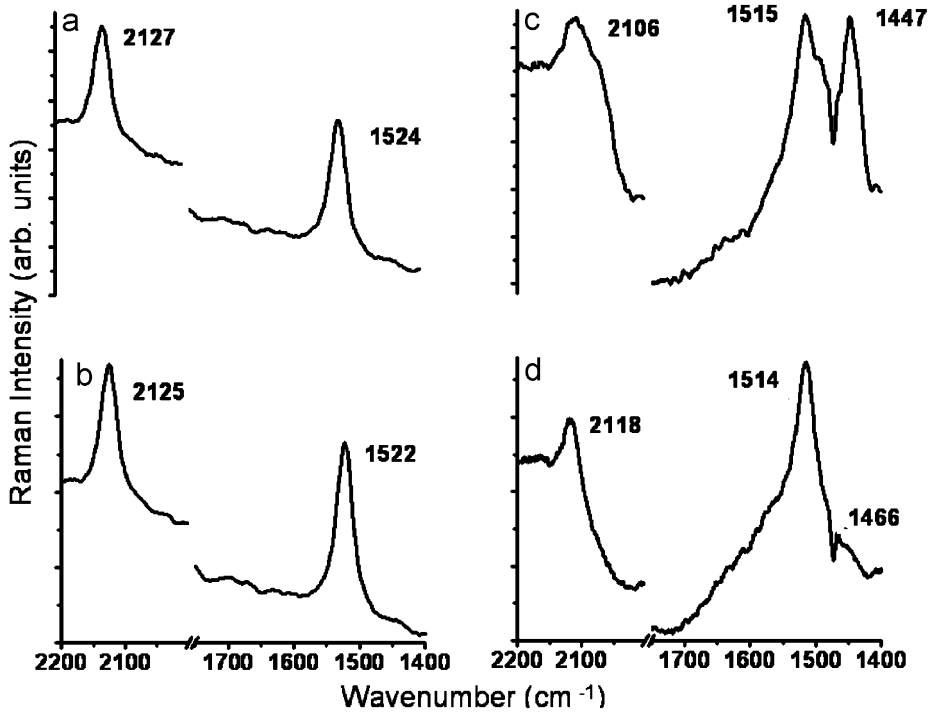

Fig. 9. Raman spectra of orange PDA–PHDAz films: (a) PDA–PHDAz reference sample, (b) PDA–PHDAz + $ZnCl_2$ 5% and preresonance Raman spectra of (c) PDA–PCDAz reference sample, and (d) PDA–PCDAz + $ZnCl_2$ 5%.

to a higher frequency within the same spectral range. Through *t*-Student statistical analysis, it was found that the mean values of the double and triple bond Raman maxima corresponding to the blue reference PDA–PCDAz films and films containing metal salt of Zn were different at a significance level of 0.05. For the band associated with the triple bond, some samples of these films with metal salt of Zn produced Raman shifts of up to 2118 cm^{-1}, outside the observed range for blue reference PDA–PCDAz samples, as is shown in Fig. 9d. In this last case, the scissoring band almost disappears, probably due to the interaction of the Zn metal salt with the blue PDA–PCDAz polymers. The shift to higher energy in the triple bond Raman signals indicates an increment of the bond order of triple bonds, which is an indication of the higher localization of the electronic cloud. As explained by Greene [40], vibration effects seem to be important for the NLO-performance of PDA materials, such effects are described by phonon mediated interactions within the material network. On the other hand, the other metal salts produced a smaller effect in the Raman signals.

3.5. Cubic NLO measurements

Finally, it was important to study the cubic NLO properties of the orange PDA–PHDAz and blue PDA–PCDAz film samples in order to clarify if the observed changes of the energetic levels were produced by the presence of the metal salts as was stated before. Due to the high conjugation of the studied PDA-polymers, high electronic mobility can be expected and the presence of different metal salts may produce strong perturbations in the delocalized π-conjugated electronic cloud. These latter properties are usually required in novel materials for the observation of NLO effects. We therefore measured the cubic NLO coefficients ($\chi^{(3)}$ values) of the selected samples according to the THG technique. THG measurements were calibrated following the standard Maker-Fringes method [41]. Experimental single beam techniques based on THG give direct access to the complex value of the non-degenerate $\chi^{(3)}(-3\omega;\ \omega,\ \omega,\ \omega)$ cubic nonlinear coefficient. One advantage of the THG technique is that the THG response accounts only for the ultra-fast electronic response, so that vibrational, orientational and thermal effects, which may contribute to the overall NLO response of the material, are excluded. By measuring the Maker-Fringes patterns of our samples, the modulus of the nonlinear coefficient can be extracted, once the nonlinear coefficient of the substrate and the linear optical constants are known. For this reason fused silica glass was chosen as NLO reference and substrate material, since its optical constants are well known and its nonlinear coefficients have been determined with high accuracy for the wavelength used in the present experiments [12,41–43]. All studied film samples were prepared with a PDA concentration greater than 95% w/w whose optical parameters were also well known. In principle, both the film and the substrate contribute to the detected THG signal (the focal length of the focusing lens used was less than 50 mm in order to make the air contribution to the THG signal

negligible [41,42]; the two contributions must be separately identified. Moreover, since the film was deposited only on one side of the substrate, the experimental configuration was asymmetric from a geometrical point of view and different relations have been developed in order to fit the 'front' configuration where the fundamental beam enters the film first, or the 'back' configuration, where the films lies behind the substrate. The equations for the interpretation of Maker-Fringes experimental patterns have been derived by several authors [43–46].

In Fig. 10, we report a typical Maker-Fringes pattern experiment (front-configuration, near-resonant configuration: $\lambda_\omega = 1064\,\text{nm}$, $\lambda_{3\omega}\sim 355\,\text{nm}$) of our best NLO orange PDA–PHDAz + $GdCl_3$ sample, deposited on a 1 mm thick fused silica glass substrate compared with the fringe pattern generated by the substrate alone. The Maker-Fringes patterns of the film-plus-substrate system, in both the P/in–P/out- and S/in–P/out-polarizing geometries, were remarkably more intense than those of the substrate alone. Due to the resonant conditions of our experiment, where the free wave was considerably absorbed by the orange PDA–PHDAz + $GdCl_3$ sample (see Fig. 2), the determination of $\chi^{(3)}$ may be approximated for film samples under resonant (absorption) conditions by the following expression [41,47]:

$$\chi^{(3)}_{\text{Film}} \propto \chi^{(3)}_{\text{S}} \left(\frac{2l^{\text{S}}_{\text{c}}}{\pi}\frac{\alpha/2}{1-\exp(-\alpha l_{\text{Film}}/2)}\right)\left(\frac{I^{\text{Film}}_{3\omega}}{I^{\text{S}}_{3\omega}}\right)^{1/2}, \qquad (1)$$

where α is the absorption coefficient of the film sample at the third harmonic (free) wave ($12.2\times10^3\,\text{cm}^{-1}$ for orange samples and $3.4\times10^3\,\text{cm}^{-1}$ for blue samples, mean values), l_{Film} represents the thickness of the film and l^{S}_{c}, represents the coherence length of the substrate (~6.2 μm). $\chi^{(3)}_{\text{Film}}$ and $\chi^{(3)}_{\text{S}}$ are, respectively, the values of the cubic nonlinear coefficients for a given film sample and the fused silica substrate, while $I^{\text{Film}}_{3\omega}$ and $I^{\text{S}}_{3\omega}$ are the peak intensities of the Maker-Fringe patterns of both the film sample and the substrate.

Since the comparison of the $\chi^{(3)}$ values between the reference PDA films and the different metal-salt based PDA film composites was an important fact to investigate, in order to verify our experimental findings, we show in Fig. 11 the calibrated NLO $\chi^{(3)}$-coefficients of selected orange PDA–PHDAz and blue PDA–PCDAz samples (SP- and PP-polarizing geometries: Figs. 11a,b, respectively), according to the Maker-Fringes method described above. A well-defined decrease of the cubic NLO coefficient was observed as the different metal-salts were added to the PDAs: for orange PDA–PHDAz samples, this decrease started from Gd ($\chi^{(3)}_{GdCl_3}\approx 2.48\times10^{-12}$ esu, $3.5\times10^{-20}\,\text{m}^2/\text{V}^2$), Eu ($\chi^{(3)}_{EuCl_3}\approx 2.21\times10^{-12}$ esu) to Zn ($\chi^{(3)}_{ZnCl_2}=1.16\times10^{-12}$ esu) for the SP-geometry and from Gd ($\chi^{(3)}_{GdCl_3}=2.42\times10^{-12}$ esu, $3.4\times10^{-20}\,\text{m}^2/\text{V}^2$), Eu ($\chi^{(3)}_{EuCl_3}=1.98\times10^{-12}$ esu) to Zn ($\chi^{(3)}_{ZnCl_2}=1.95\times10^{-12}$ esu) for the PP-geometry. A similar trend for blue PDA–PCDAz

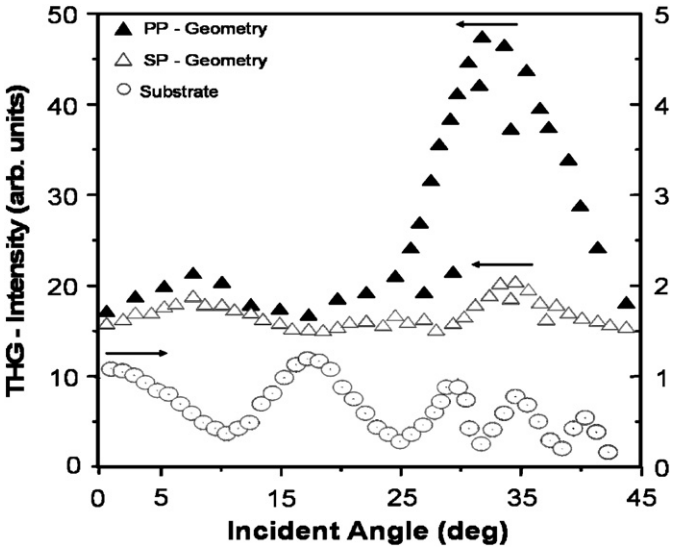

Fig. 10. Angle dependent THG measurement performed on the P + $GdCl_3$ sample and the reference substrate (PP- and SP-polarizing geometries).

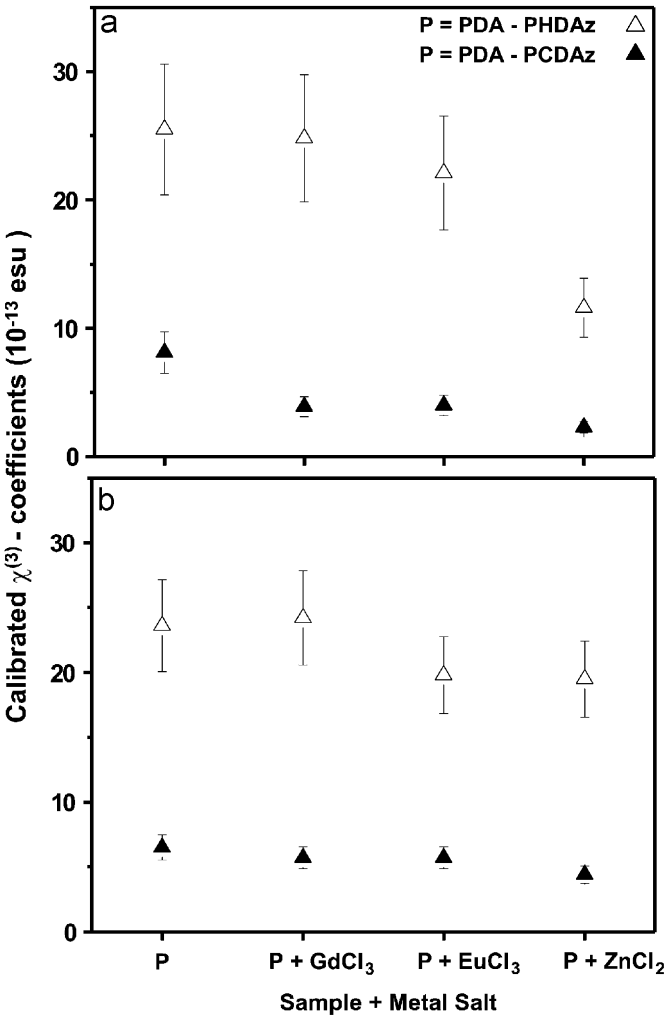

Fig. 11. $\chi^{(3)}$ values of orange PDA–PHDAz and blue PDA-PCDAz films: (a) SP-polarizing geometry and (b) PP-polarizing geometry. An estimated error of about 20% is considered.

samples, in both, the SP-, and PP-polarizing geometries was observed, but the variation effect (in %) of the metal salts on the $\chi^{(3)}$ value was larger. It was also found that the metal salt of Zn induced the smallest $\chi^{(3)}$ value for both the orange and blue film samples (SP- and PP-polarizing geometries). Furthermore, in the case of blue PDA–PCDAz films, cascading effects were detected and the degenerated $\chi^{(3)}(-3\omega;\ 2\omega,\ \omega)$ coefficient was also present. It is well known that lower-order optical nonlinearities may contribute in multi-step or cascade fashion to higher-order nonlinear phenomena [48]. Since the blue PDA–PCDAz samples showed high absorption in the blue-green region, the $\chi^{(3)}$ shows typical resonant enhancements when either the energy of the photons at fundamental frequency, or at the second harmonic (SHG, $\lambda_{2\omega} = 532\,\text{nm}$) or THG frequencies, approach the energy of the real transition in the material [49–51]. Correspondingly, one can talk of single-photon, two-photon and three-photon resonances, considering the double (2ω) and single (ω) frequency expressed by sum over states (SOS approach). In particular, the $\chi^{(3)}(-3\omega;2\omega,\omega)$ degenerated coefficients measured for blue PDA–PCDAz samples were in any case smaller than the dominant $\chi^{(3)}(-3\omega;\ \omega,\ \omega,\ \omega)$, cascading-free, three photon resonance coefficients, observed for orange PDA–PHDAz films.

In the evaluation of the cubic $\chi^{(3)}$ values for the orange PDA–PHDAz and blue PDA–PCDAz reference films according to THG measurements, it was found that they were almost equal for both the SP- and PP-implemented polarizing geometries. However, as the metal salts were added, the SP-configuration gave maximal variation of the $\chi^{(3)}$ coefficients by the interaction of the PDAs with the metal salts. This indicates that the metal salt made the electronic cloud more localized and, in general, the higher $\chi^{(3)}$ response was in the same direction as that of the incident fundamental beam polarization (PP-polarizing geometry, in this case). The largest $\chi^{(3)}$-values found for the orange PDA–PHDAz samples are attributed to the higher concentration of PDAs in these films and probably to the increase of the delocalization of the π electron system, caused by the allylic ester groups [52]. This increase of delocalization also caused a greater asymmetry of the π-conjugated cloud, which provoked some forbidden transitions to become allowed and hence, the absorption- and the $\chi^{(3)}$-coefficients could be increased. This latter phenomenon became more relevant for THG experiments, where more energy levels were involved. The $\chi^{(3)}$-values of orange PDA–PHDAz and blue PDA–PCDAz reference films in the SP-polarizing geometry were 2.55×10^{-12} esu ($3.6\times10^{-20}\,\text{m}^2/\text{V}^2$) and 0.81×10^{-12} esu ($1.1\times10^{-20}\,\text{m}^2/\text{V}^2$), respectively. The lower values of these films compared to those reported by Ogawa et al. (10^{-10} esu) [27] are explained by the resonant conditions ($\lambda_{\text{incident}} = 532\,\text{nm}$) used in that work and the different structures of the polyesters. In these experiments Ogawa et al. implemented the degenerate four-wave mixing (DFWM) technique, which usually gives lower precision to the evaluated nonlinearities. Other important and earlier works performed on NLO properties of PDA systems have been reported by Dennis et al. and by Carter et al. [53,54]. In the first case, moderated saturated solutions of orange and red PDAs containing-polyesters in chloronaphthalene were studied implementing the DFWM technique, using ps-laser pulses at low repetition rate and at $\lambda_{\text{incident}} = 532\,\text{nm}$. Under these experimental conditions $\chi^{(3)}_{xyyx}$ values in the order of $(7\pm2)\times10^{-12}$ esu were estimated for the studied PDA samples [53], which are of the same order of magnitude as those reported in this work. In the second case [54], DFWM experiments using ps-dye laser pulses were also performed in high quality single PDAs organic crystals, where both time and wavelength resolved NLO measurements were performed. In these experiments, a fast response time of the order of 6 ps and $|\chi^{(3)}|$ magnitudes of the order of 9×10^{-9} esu (at $\lambda_{\text{incident}} = 651.5\,\text{nm}$) and 5×10^{-10} esu (at $\lambda_{\text{incident}} = 701.5\,\text{nm}$) were, respectively, obtained for the solid state samples. In last case, the higher cubic NLO values obtained through the dispersion study performed with the dye-laser, originates from the highly ordered crystalline structure of these samples.

In the present study, we argue that the decrease of the NLO response of these polymers caused by the metal salts is due to the presence of cations and anions, which interfere with the delocalization of the electronic cloud of PDAs. Lower variations of the $\chi^{(3)}$ values appeared for the orange PDA–PHDAz films and are attributed to the increment of the delocalization of the π electrons when the metal ion was coordinated with the carbonyl of the ester groups in allylic position to the enynes as probably occurred in the orange PDA–PHDAz films. The larger effect of the Zn metal is explained in terms of the d^{10} configuration of the Zn^{2+} cation where the d orbitals are full and, therefore, interfere more strongly in the delocalization of the electronic cloud of PDAs. In addition, the effective nuclear charge (Z) of the Zn^{2+} cation and its ionic radius r produced a higher ionic potential $\phi = Z/r$) [55] than Eu^{3+} and Gd^{3+} and then its perturbation on the electronic cloud polarization of PDAs was larger. This phenomenon was different to the addition of $Co_2(CO)_6$ to PDAs [14], where a bonding between the Co and PDAs π orbitals was formed, which increased the $\chi^{(3)}$ values. In our case, however, the addition of metal salts of Zn, Gd and Eu did not produce organometallic bonding between the cation and the π bonds of PDA-containing polyesters, rather only an electrostatic effect in the π bonds is observed.

4. Conclusions

The addition of metal salts to PDA-containing polyesters films provoked the interaction of the metal salts with the conjugated system and ester groups of these polymers. It was found that the conjugated bonds became more localized by this interaction. Indeed, if the ester group was in allylic position, the interaction of the metal ion with the carbonyl group increased the conjugation. It was realized

that the electronic cloud localization could affect the PDAs polarizability and in consequence their NLO properties. Through THG measurements, this hypothesis was verified and the $\chi^{(3)}$ values were unfortunately decreased by the interaction of PDAs with the metal salts, where localized electronic clouds were sensitively detected by NLO measurements. However, this decrement was smaller when the metal interacted with the carbonyl group of the allylic ester to the conjugated system, because this interaction increments the conjugation of this system. On the other hand, it was possible to correlate shifts to higher energy in UV-absorption and Raman measurements with a higher localization of the electronic cloud and consequently with a decrement of the NLO properties. In addition, the PL measurements indicate a decrement of the emission intensity of PDAs due to the presence of the metal salts; this indicates an increment of the non-radiative decay from the vibronic energy levels, which is also related to a decrement of the NLO properties. In other words, it was found that the STE formation in PDAs was also affected by the interaction of the metal salts.

Acknowledgments

We gratefully acknowledge technical support from M.A. Canseco (DSC measurements), L. Huerta (XPS measurements), L. Baños (WAXS measurements), G. Cedillo (GPC measurements), C.Flores (PL measurements) and M. Bizarro (perfilometry measurements); S.E. Castillo-Blum, R. Martínez-Martínez, S.E. Rodil, M. Hipólito-García, E. Cervera and M.E. Sosa-Torres for commentaries to this article. Neil Bruce for English revision and C.J. Roman-Moreno (CCADET-UNAM) for valuable technical assistance and laser maintenance. One of the authors (O.G. Morales-Saavedra) gratefully acknowledges the financial support of SEP-CONACyT-México under project Grant 47421. J. A. Díaz-Ponce gratefully acknowledges for the CONACYT scholarship and support from the Postgraduate Department of the Instituto de Investigaciones en Materiales, UNAM.

References

[1] M. Yoshizawa, A. Yasuda, T. Kobayashi, Appl. Phys. B 53 (1991) 296.
[2] S.D.D.V. Rughooputh, D. Bloor, D. Phillips, R. Jankowiac, L. Schütz, H. Bässler, Chem. Phys. 125 (1988) 355.
[3] R. Lécuiller, J. Berréhar, C. Lapersonne-Meyer, M. Schott, Phys. Rev. Lett. 80 (1998) 4068.
[4] D. Comoretto, I. Moggio, C. Cuniberti, G. Dellepiane, Synth. Met. 94 (1998) 229.
[5] M. Yoshizawa, A. Kubo, S. Saikan, Phys. Rev. B 60 (1999) 15632.
[6] J. Olmsted III, M. Strand, J. Phys. Chem. 87 (1983) 4790.
[7] J.S. Salafsky, Phys. Rev. B 59 (1999) 10885.
[8] S. Musikhin, L. Bakueva, E.H. Sargent, A. Shik, J. Appl. Phys. 91 (2002) 6679.
[9] N.C. Greenham, X. Peng, A.P. Alivisatos, Phys. Rev. B 54 (1996) 17628.
[10] H. Okawa, M. Sekiya, J. Osawa, T. Wada, A. Yamada, H. Sasabe, T. Uryu, Polym. J. 23 (1991) 147.
[11] A.K. Kar, Polym. Adv. Tech. 11 (2000) 553.
[12] H.S. Nalwa, in: H.S. Nalwa, S. Miyata (Eds.), Nonlinear Optics of Organic Molecules and Polymers, CRC Press, Florida, 1997 (Chapter 10–12).
[13] N.J. Long, in: D.M. Roundhill, J.P. Fackler (Eds.), Optoelectronic Properties in Inorganic Compounds, Plenum Press, New York, 1999 (Chapter 4).
[14] N.M. Agh-Atabay, W.E. Lindsell, P.N. Preston, P.J. Tomb, A.D. Lloyd, R. Rangel-Rojo, G. Spruce, B.S. Wherrett, J. Mater. Chem. 2 (1992) 1241.
[15] H.S. Zhou, T. Wada, H. Sasabe, H. Komiyama, Synth. Met. 81 (1996) 129.
[16] H.S. Zhou, T. Wada, H. Sasabe, Chem. Soc. Chem. Commun. (1995) 1525.
[17] T. Ogawa, et al., unpublished results.
[18] W.Y. Xu, Y.S. Wang, D.G. Zheng, S.L. Xia, J. Macromol. Sci. Chem. A 25 (1988) 1397.
[19] E. Banks, Y. Okamoto, Y. Ueba, J. Appl. Polym. Sci. 25 (1980) 359.
[20] Y. Okamoto, J. Kido, H.G. Brittain, S. Paoletti, J. Macromol. Sci. Chem. A 25 (1988) 1385.
[21] L.A. Belfiore, M.P. McCurdie, J. Polym. Sci. Part B 33 (1995) 105.
[22] P.K. Das, I. Ruzmaikina, L.A. Belfiore, J. Polym. Sci. Part B 38 (2000) 1931.
[23] M. Jiang, C. Zhou, Z. Zhang, Polym. Bull. 30 (1993) 455.
[24] G. Petersen, A. Brodin, L.M. Torell, M. Smith, Solid State Ionics 72 (1994) 165.
[25] J. Tang, C.K.S. Lee, L.A. Belfiore, J. Polym. Sci. Part B 41 (2003) 2200.
[26] L.A. Belfiore, M.P. McCurdie, Polym. Eng. Sci. 40 (2000) 738.
[27] S. Fomine, E. Adem, T. Ogawa, D.V.G.L.N. Rao, Polym. Bull. 34 (1995) 169.
[28] S. Fomin, R. Neyra, T. Ogawa, Polym. J. 26 (1994) 845.
[29] A.R. Moreno, J.G. Robledo, A.M. Mendoza, M.F. Beristaín, T. Ogawa, Rev. Soc. Quim. Mex. 46 (2002) 32.
[30] A.S. Hay, J. Org. Chem. 27 (1962) 3320.
[31] X. Hu, X. Li, J. Polym. Sci. Part B 40 (2002) 2354.
[32] R.E. Southward, D.S. Thompson, D.W. Thompson, A.K.S. Clair, in: C.U. Pittman Jr., C.E. Carraher, M. Zeldin Jr., J.E. Sheats, B.M. Culbertson (Eds.), Metal-containing Polymeric Materials, Plenum Press, New York, 1996, pp. 337–347.
[33] T. Kimura, R. Nagaishi, Y. Kato, Z. Yoshida, J. Alloys Compds. 323–324 (2001) 164.
[34] O.P. Dimitriev, V.V. Kislyuk, Chem. Phys. Lett. 377 (2003) 149.
[35] B.C. Roy, M.A. Fazal, A. Arruda, S. Mallik, A.D. Campiglia, Org. Lett. 2 (2000) 3067.
[36] J. Guillet, Polymer Photophysics and Photochemistry, Cambridge University Press, Cambridge, 1987 (Chapters 7, 10).
[37] E.I. Rashba, M.D. Sturge (Eds.), Excitons Selected Chapters, North-Holland, Amsterdam, 1987 (Chapters 1, 7).
[38] A.M. North, D.A. Ross, J. Polym. Sci. Symp. 55 (1976) 259.
[39] D.N. Batchelder, D. Bloor, in: R.J.H. Clark, R.E. Hester (Eds.), Advances in Infrared and Raman Spectroscopy, Wiley-Heyden, Chichester, 1984 (Chapter 4).
[40] B.I. Greene, J.F. Mueller, J. Orenstein, D.H. Rapkine, S. Schmitt-Rink, M. Thakur, Phys. Rev. Lett. 61 (1988) 325.
[41] F. D'Amore, A. Zappettini, G. Facchini, S.M. Pietralunga, M. Martinelli, C. Dell'Erba, C. Cuniberti, D. Comoretto, G. Dellepiane, Synth. Met. 127 (2002) 143.
[42] B. Buchalter, G.R. Meredith, Appl. Opt. 21 (1982) 3221.
[43] F. Kajzar, J. Messier, Phys. Rev. A 32 (1985) 2352.
[44] X.H. Wang, D.P. West, N.B. McKeown, T.A. King, J. Opt. Soc. Am. B 15 (1998) 1895.
[45] K. Miyano, T. Nishiwaki, A. Tomioka, Opt. Commun. 91 (1992) 501.
[46] D.S. Bethune, J. Opt. Soc. Am. B 6 (1989) 910.
[47] H. Nakanishi, H. Matsuda, S. Okada, M. Kato, Polym. Adv. Tech. 1 (1990) 75.

[48] G.R. Meredith, Phys. Rev. B 24 (1981) 5522.
[49] R.W. Boyd, Nonlinear Optics, Academic Press, San Diego, 2002.
[50] J.F. Ward, Rev. Mod. Phys. 37 (1965) 1.
[51] P.A. Chollet, F. Kajzar, J. Messier, Synth. Met. 18 (1987) 459.
[52] J.B. Armitage, M.C. Whiting, J. Chem. Soc. Part II (1952) 2005.
[53] W.M. Dennis, W. Blau, D.J. Bradley, Appl. Phys. Lett. 47 (1985) 200.
[54] G.M. Carter, M.K. Thakur, Y.J. Chen, J.V. Hryniewicz, Appl. Phys. Lett. 47 (1985) 457.
[55] J.E. Huheey, E.A. Keiter, R.L. Keiter, Inorganic Chemistry, Harper Collins College Publishers, New York, 1993, pp. 129–131.